A new approach to numerical characterisation of wear particle surfaces in three-dimensions for wear study

Y. Tian[a,*], J. Wang[b,*], Z, Peng[c], X. Jiang[b]

**. These authors contributed equally to this work.*

a. School of Engineering and Physical Sciences, James Cook University, Townsville, QLD 4811, Australia

b. Centre for Precision Technologies, School of Computing and Engineering, University of Huddersfiled, Huddersfield, HD1 3DH, UK

c. School of Mechanical & Manufacturing Engineering, The University of New South Wales, Sydney, NSW 2052, Australia

Abstract

In the wear and tear process of synovial joints, wear particles generated and released from articular cartilage within the joints have different surface topology and mechanical property. Three-dimensional (3D) particle images acquired using laser scanning confocal microscopy (LSCM) contain appropriate surface information for quantitatively characterizing the surface topology and changes to seek a further understanding of the wear process and wear features. This paper presents a new attempt on the 3D numerical characterisation of wear particle surfaces using the field and feature parameter sets which are defined in ISO/FDIS 25178-2. Based on the innovative pattern recognition capability, the feature parameters are, for the first time, employed for quantitative analysis of wear debris surface textures. Through performing parameter classification, ANOVA analysis and correlation analysis, typical changing trends of the surface transformation of the wear particles along with the severity of wear conditions and Osteoarthritis (OA) have been observed. Moreover, the feature parameters have shown a significant sensitivity with the wear particle surfaces texture evolution under OA development. A correlation analysis of the numerical analysis results of cartilage surface texture variations and that of their wear particles has been conducted in this study. Key surface descriptors have been determined. Further research is needed to verify the above outcomes using clinic samples.

Keywords: Wear particles, Numerical characterisation, Field and feature parameters, Surface topography, Osteoarthritis diagnostics

1. Introduction

Osteoarthritis (OA) is a joint degeneration disease, which commonly affects majority people over certain age groups [1, 2]. It is also one of the top leading disability diseases with advanced OA normally resulting in a total joint replacement operation [3-5]. Early diagnosis and intervention is essential which would both improve patients' life quality and save a significant amount of public health fund [6]. Articular cartilage within a synovial joint has a layered, inhomogeneous structure which could be classified into the superficial, transitional, middle or deep zone and the calcified cartilage [7-10]. During OA process, the integrity of cartilage is suffering a continuous loss, accompanied with abrasion and fissure reaching down to the deep and calcified cartilage region. Accordingly, OA severity could be defined into grades 1 to 3 based on the loss of total cartilage thickness [1, 11, 12].

Wear debris, the by-products of the above wear process, contains valuable information in its surface topography and mechanical properties for assisting in the understanding of OA mechanisms and wear features. For example, it has been revealed, from previous qualitative studies [12-15], that particles generated in a healthy joint normally have a lamellar shape. Generation and detection of chunky or osseous fragments indicate that the wear condition deteriorates into calcified or subchondral regions. Therefore, study of the morphology of wear particles from a synovial joint could reveal the wear process and condition relating to their origination [15-17]. Since synovial fluid extraction is an easy process, wear particles study could offer an alternative and convenient approach compared with conventional OA diagnostic techniques based on cartilage evaluation using radiography, magnetic resonance imaging and arthroscopy, etc [7, 18-23].

In the past 15 years, the study of wear particles for OA study has attracted interests. The wear particles analysis technique using numerical descriptors has been recognized as an objective and non-destructive approach for OA

assessment. However, due to the restrictions of the microscopy techniques used, conventional boundary morphologies have been mainly investigated based two-dimensional (2D) information acquired using Scanning Electronic Microscopy (SEM) [12-15, 24]. However, standard SEM is not a suitable facility for obtaining appropriate surface data for 3D surface analysis due to a number of factors including its 2D nature, sample preparation requirement prior to imaging, and surface dehydration and resulted artefacts in the imaging process.

The development and application of Laser Scanning Confocal Microscopy (LSCM) to the wear particles study has enabled a possible advancement in 3D quantitative analysis of wear particles generated in a synovial joint. LSCM has the ability to acquire high resolution images by transmitting specimen information back through the optics via a confocal aperture to reduce light from above and below focal plane. Once a series of sequential 2D slices is captured at different heights in the specimen, 3D images can be complied providing 3D surface and volume information. LSCM has a number of advantages including having a higher resolution than a standard stylus profiler, requiring minimal sample preparation and being a fast, non-intrusive and versatile instrument for quantitative surface measurement [25-29]. Owning to its advantages, LSCM has been used to capture 3D surface information of specimens in engineering and bio-engineering field [30-32].

For surface characterisation, it has been known that all surfaces have small-scale geometrical information that is usually called surface topography [33]. The surface topography information records the creation history of the material and from which, the functionality and lifetime of the material can be predicted quantitatively. Based on the development of mathematical and engineering parameters, certain efforts have been implemented to numerically characterise the surface texture information of both cartilage and particles under OA progression [30, 34-37]. However, an effective wear particles analysis technique is yet to be developed as a non-destructive tool for OA study and potential wear prediction.

In the numerical characterisation discipline, profile (2D) characterisation tools are phased out [38] as the surface metrology on areal characterisation of surface texture is progressing rapidly. The novel feature characterisation techniques [39] have been introduced into engineering measurements, and the "field parameters" and "feature parameters" have been proposed in the international standard ISO/FDIS 25178-2 [40]. Specifically, the field parameters directly apply statistics to the continuous surface data (cloud of points). The feature parameters carry out statistics to a subset of predefined topographic features. Some pattern recognition techniques such as the "hill and valley recognition", "edge detection" and "Wolf prune" are involved so that the surface features can be characterised using these parameters [41-43]. By means of the advanced surface characterisation techniques [42, 44], comprehensive surface topographies of wear particles can be investigated for wear analysis and OA diagnostics.

This research, in parallel with the 3D numerical characterisation of articular cartilage surfaces [49], is for the first time to apply feature parameters to evaluate the functional properties of surface topography of wear particles from sheep synovial joints. By applying both the field and feature parameter sets in the particle surface topography assessment, comprehensive surface information has been analysed. Changes in the wear particles surface topography with the wear process have been observed after performing parameter classification, ANOVA analysis and correlation analysis. Because the wear particles came from the cartilages surfaces in the wear processes, a correlation between the significant parameters of the particle surfaces and the cartilages surfaces have also been carried out. A set of key parameters, i.e., the most significant numerical descriptors which are able to reveal the surface evolutions, are determined as potential indicators for monitoring changes in the wear conditions.

2. Experimentation and Image Acquisition

To collect wear particles samples for the proposed surface studies, synovial fluids were collected from sheep knee joints which were tested on a designated apparatus to generate worn cartilage and particles samples in Osteoarthritis (OA) degrees 1 to 3. The synovial fluid samples were processed for fixation and wear particles were acquired through the filtergram method. Then the wear particles samples were fluorescent stained and imaged using laser scanning confocal microscopy (LSCM). A series of images stacks containing three-

dimensional (3D) surface information was compiled to form the height encoded image for the numerical analysis to be presented in section 3. Detailed information on the wear tests, sample collection and imaging process is presented below.

2.1. Wear test

To investigate wear features and conditions in synovial joints for OA understanding and assessment, various engineering configurations including wear simulators have been established to simulate real tribological environment and generate desired degrees of wear conditions [45-47]. The wear simulator which has been designed and constructed at the Mechanical Engineering workshop, James Cook University (JCU), Australia, was used to perform wear testing on sheep knee joints. The equipment simulates walking process with various loads supplied by a pneumatic air bag system [30].

Since human and sheep knee joints have been confirmed to have similar properties when undergoing wear process [48, 49], wear particles samples from sheep knee joints were used in this study. Synovial fluid samples containing wear particles were harvested from the knee joints of six sheep hind legs. Complied with the JCU animal ethical approval for this project, three 11 months old merino sheep were euthanized, and all sheep legs were tested within 12 hours after the euthanasia. One joint without being subjected to the wear testing was used as the control joint in a healthy condition. The other five joints were tested in various durations ranging from one and half hours to more than 11 hours so the desired OA grades could be achieved [30, 37]. Table 1 shows the testing conditions and corresponding OA grades of the tested knee joints.

Table 1 Joint wear test conditions [30].

Joint No.	Load (kg)	Testing Cycles	OA Degree
Control	0	0	0
Joint 1	15	10,000	1
Joint 2	15	12,000	1,2
Joint 3	15	17,000	2
Joint 4	15	26,000	2,3
Joint 5	15	37,000	3

2.2. Wear particles samples collection

Once a wear test was completed, 10 ml saline solution was injected into the joint sack and all legs were flexed and stretched a few times for uniformly mixing with synovial fluid. Due to tissue water-absorption, normally less than 5 ml liquid was extracted using a syringe. During the extraction, particularly caution must be exercised to ensure the syringe needle not to contact the cartilage surface. The collected synovial fluid was mixed with 2% glutaraldehyde and then stored in a 4℃ fridge over 24 hours for fixation. Before imaging, wear particles suspended in the synovial fluid were fluorescent stained with 0.03g/L Rodamine B solution and then separated using the filtergram method with a 3 μm pore sized membrane. The filter paper with the collected particles was transferred to a glass slide with a drop of clarifying solution designed to make the filterpaper transparent for an easy observation and imaging of the wear particles. The wear particles were ready for imaging using LSCM.

2.3. LSCM imaging & processing

An Argon laser with 515/30 nm emission filter was chosen to capture the images of the stained wear debris as the Rodamine B has a maximum absorbance at 553nm [50]. The wear particles were imaged with a 100x objective lens to achieve an appropriate magnification capacity. All images encompassed 512*512 pixels and were scanned with a 0.15 μm step size in the z-direction. For each joint sample, 15 wear particles were preliminarily imaged. A further exclusion was performed to ensure that only images with appropriate boundary and surface information

suitable for numerical characterisation were selected for the next phase of the project, that is, the quantitative analysis of the boundary and surface topography of the wear particles. In average, about 10 particles from each joint were selected.

Before conducting the numerical analysis, which will be detailed in the following section, 2D image stacks captured using the LSCM were compiled to generate a pair of images using the MatLab codes developed at JCU, Australia [30]. The pair of images is high encoded image and maximum brightness image. The height encoded image, which stores 3D data, is suitable for 3D surface characterisation using the field & feature parameters.

3. Quantitative Image Characterisation Techniques

For quantitative surface measurements, there are over thirty numerical parameters suggested in the International Organization for Standardization (ISO) standard [40]. Both field and feature parameters have been used in this study to characterise the surface morphology of the wear particles while their boundary properties have also been quantitatively analysed.

3.1. Pre-processes

Surface topography is usually multi-banded, which means that it is comprised of many spectral ingredients with different wavelengths. Filtration to prune out the unexpected spectrum is usually the first step for numerical characterisation. The new international standard ISO 25178-3 [51] has suggested the S-L filtration with specific nesting indices, i.e. filtering cut-off, for general surface texture characterisation. The nesting indices of the filtering process are usually determined by the size of the interesting features, the radius of the employed scanning tip and sampling settings, etc.

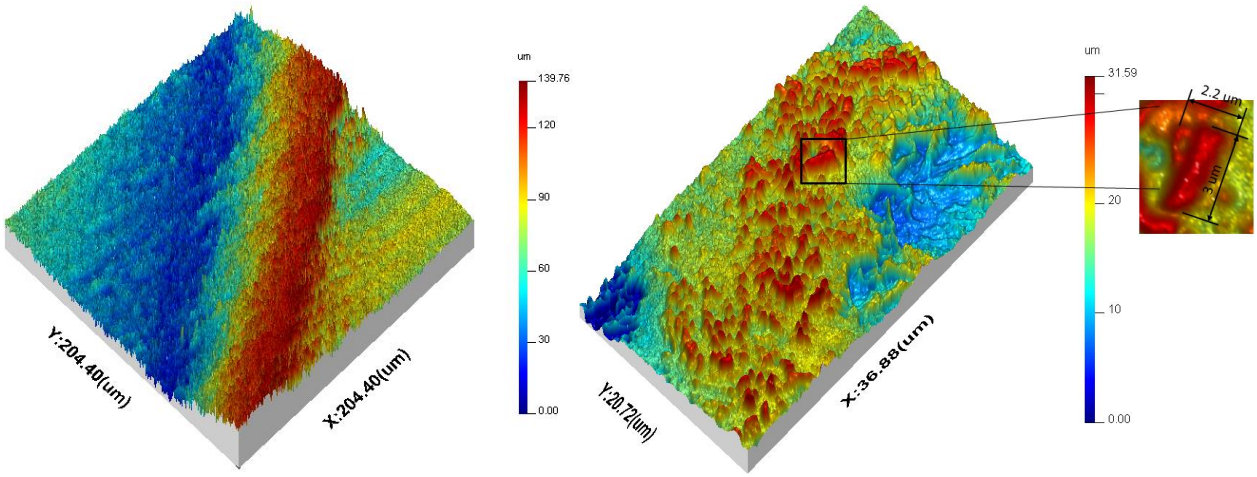

(a) (b)

Fig. 1. (a) A measurement of an articular cartilage surface; and (b) A measurement of a wear particles surface generating in the same knee joint of the cartilage sample.

Table 2 The sampling conditions and the selected nesting indices of S-L filtration in this experiment.

Sampling spacing	S-filter nesting index	Sampling length	F-Operator	L-filter nesting index
0.16 μm	0.8 μm	82 μm	Levelling	8 μm

In the parallel project on the numerical analysis of articular cartilages [52], the nesting indices of S-L filtration [40] were set to be 2.5 μm – 25 μm based on the fact that the size of the interesting features are within the range. Fig. 1(a) shows a typical measurement result of an articular cartilage surface. As for the wear particles surface topography in this research, the experimental investigations reveal that the size of most of the wear debris is on

the micro-metre scale ranging from 8 μm – 45 μm while the size of interesting surface features usually falls in 0.8 μm to 3.6 μm. A randomly selected measurement result is illustrated in Fig. 1(b). Referring to the suggested filtration nesting indices, the 0.8 μm – 8 μm S-L filtration with Gaussian filters [51, 53] has therefore been employed on the surface topography data of the wear particles to remove unwanted information. Table 2 shows the details o the selected nesting indices of the S-L filtration for the wear debris. Because the sizes of the particles are usually smaller than the measuring window (sampling length-determined), the surrounding background regions which are usually smooth needed to be clipped. Fig. 2 illustrates a series of typical processed results (filtration and clipping) of the control sample to Joint 5. The processed images are then analysed using the numerical parameters.

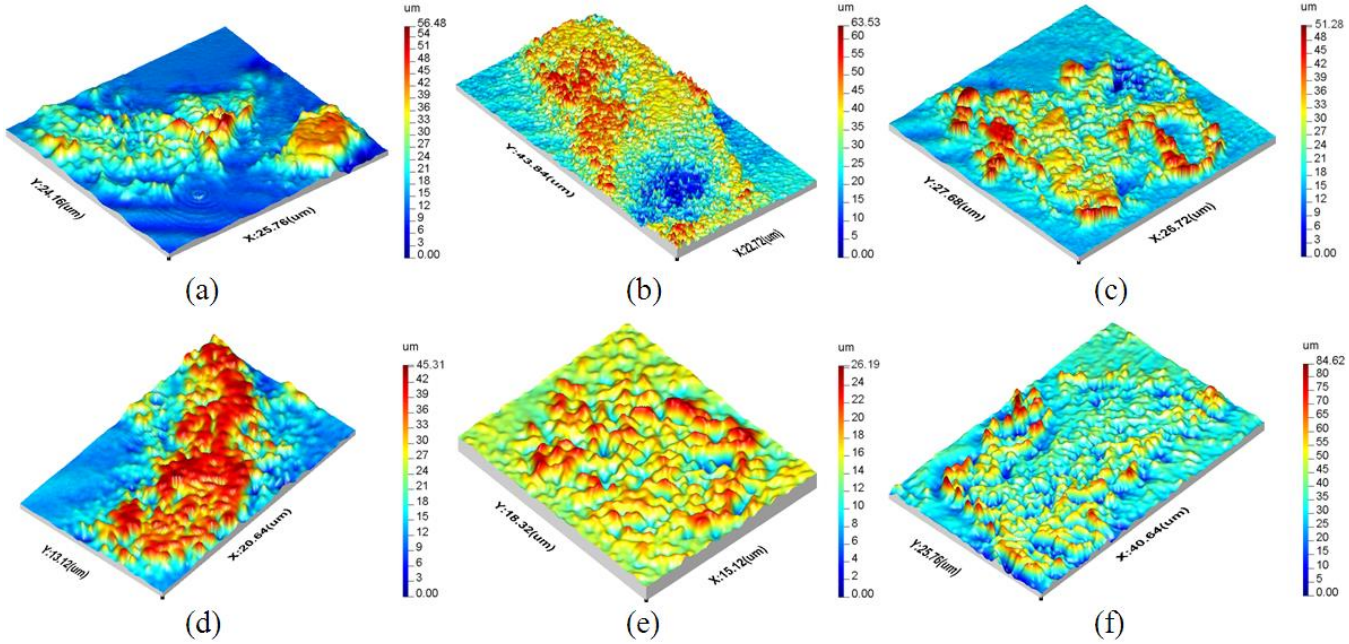

Fig. 2. Illustration of the representative measurement results of the 6 sample groups (a) Control; (b) Joint 1; (c) Joint 2; (d) Joint 3; (e) Joint 4; and (f) Joint 5 after filtering.

3.2. Numerical analysis

Areal surface topography characterisation was carried out to reveal the surface roughness morphology of wear particles under OA development. To make the results comparable with former researches, a boundary morphology numerical study was also implemented to examine the shape complexity of the wear particles.

Boundary Characterisation

Representative boundary parameters including area, length, aspect ratio, roundness, curl, convexity, formfactor and fractal dimensions were calculated and are listed in Table 3. From the values, it can be seen that the boundary morphology of the particles alters during the wear process. Wear particles are averagely sized around 50 μm length and a few thousands of μm^2 dimensions. From control joint to joint 4, both debris area and length perform an initial increase and then decrease trend, followed by suddenly rise at last severe worn joint. Meanwhile, other parameters such as convexity and fractal dimensions are slightly fluctuating, which means the form of wear particles remain steady during wear testing process.

Table 3 Average values of the boundary parameters for the wear particles.

Parameters	**Control**		**Joint 1**		**Joint 2**		**Joint 3**		**Joint 4**		**Joint 5**	
	Mean	S. D.	Mean	S. D.	Mean	S. D.	Mean	S. D.	Mean	S. D.	Mean	S. D.
Area (μm^2)	855	699	1570	1120	1609	1109	1414	842	1026	922	2404	1467

Length (μm)	40	19	57	23	57	21	54	19	47	20	65	21
Aspect Ratio	1.44	0.28	1.37	0.31	1.38	0.26	1.41	0.23	1.61	0.52	1.19	0.17
Roundness	0.64	0.12	0.60	0.13	0.59	0.11	0.59	0.11	0.54	0.13	0.68	0.10
Curl	572	69	567	64	557	71	547	76	595	67	532	48
Convexity	0.83	0.02	0.82	0.03	0.80	0.02	0.81	0.03	0.83	0.02	0.82	0.02
Formfactor	0.57	0.07	0.52	0.08	0.51	0.08	0.52	0.09	0.52	0.07	0.56	0.06
Fractal Dimensions	1.102	0.013	1.106	0.012	1.107	0.011	1.107	0.015	1.103	0.018	1.102	0.008

Surface Characterisation

It has been stated, in ISO 25178-2, that the field parameters are used to classify averages, deviations, extremes and specific features on a scale-limited continuous surface [40]. These parameters have some limitations. Innovatively defined feature parameters apply statistics to a subset of predefined topographic features which are usually extracted using the pattern recognition techniques such as the "hill and valley detection" [41], "edge detection" [54] and "Wolf pruning" [43]. Some feature parameter applications in engineering disciplines have shown their significant advantageous [41, 54, 55]. These two parameter sets with a total of thirty-two numerical parameters have been applied to analyse the wear particles using the SURFSTAND [44]. The thirty-two parameters are listed in Table 4. Due to the large amount of raw data generated in the surface analysis, only the results of selected key parameters will be presented in Section 4.

Table 4 The thirty-two areal surface texture parameters classifications.

Height related							**Spatial**				**Hybrid**		
Peak height	Valley height	Core height	Total height	Mean height	Skewness	Kurtosis	Aspect ratio	Feature area	Feature density	Correla-tion length	Feature volume	Gradient	Curvature
Sp	*Sv*	*Sk*	*Sz*	*Sq*	*Ssk*	*Sku*	*Str*	*Sda*	*Spd*	*Sal*	*Sdv*	*Sdr*	*Spc*
Spk	*Svk*	*Vmc*	*S10z*	*Sa*				*Sha*			*Shv*	*Sdq*	
Smr	*Sxp*	*Vvc*											
Smc	*Smr2*												
Smr1	*Vvv*												
Vmp	*S5v*												
S5p													

Note: Yellow highlighted are the feature parameters.

4. Data Analysis and Key Results

In most of cases, many parameters have less or no direct relations with the interesting functionalities such as broad-spectrum absorption, self-cleaning or the osteoarthritis (OA) diagnostics in this research. In addition, many parameters usually have close description capabilities due to their similar physical definitions. For example, *Sp*, *S5p* and *Spk* all describe the geometric properties related to the peaks within a surface; both *Sa* and *Sq* describe the general height deviations within a surface and they are highly correlated. It is necessary to find out the most significant parameters (called key parameters in this study) which have the most significant and stable relations to the anticipated functionalities. As introduced earlier, a parameter classification, combined with an ANOVA and correlation analysis, are innovatively carried out here.

4.1 One-way ANOVA and parameter classification

To evaluate the significance of the 32 numerical parameters in extracting distinctive features of the wear particles, an one-way ANOVA [56] was carried out. By selecting p=0.05 as the critical level, 23 parameters have been

revealed to be significant for the wear particles characterisation. It is worth to mention that 8 of total 9 feature parameters, highlighted in Table 5, have shown significance.

Table 5 Classification of the twenty-three significant parameters by their definitions with the highlighted key feature parameters in yellow.

Height related					**Spatial**		**Hybrid**	
Peak height	Valley height	Core height	Total height	Mean height	Feature area	Feature density	Feature volume	Gradient
Sp	*Sv*	*Sk*	*Sz*	*Sq*	*Sda*	*Spd*	*Sdv*	*Sdr*
Spk	*Svk*	*Vmc*	*S10z*	*Sa*	*Sha*		*Shv*	
Smc	*Sxp*	*Vvc*						
Vmp	*Vvv*							
S5p	*S5v*							

For further significance test, correlation to prune out those redundant parameters is usually employed [30]. Prior to the correlation process, a classification of the total parameters based on their definitions is needed. Referred to Table 5, the 23 significant parameters can be classified into three widely accepted parameter types, namely, height-related (or amplitude), spatial and hybrid parameters [57, 58]. The height-related parameters are those who only or mainly depend on the surface height deviations. The spatial parameters refer to the spacing of certain topographic features while the hybrid parameters make equal use of the information contained in the elevations and spatial positions [58]. The height related parameters can be further classified into five sub-categories (shown in Table 5) with the parameters in each group having close describing capabilities. For example, *Sp*, *Spk*, *Smc*, *Vmp* and *S5p* are all relevant to the height of the peak features within a surface. Similarly, the parameters in the spatial and hybrid group have also been divided into two sub-groups based on which feature the parameters can characterise.

4.2 Three typical trends

Based on the calculations and analyses conducted in the former sessions, three typical, non-monotonic trends of the surface topographic parameters have been observed with increasing wear cycles. They are Types 1, 2 and 3 as shown in Fig. 3 (blue lines) which are represented by the height parameter *Sp* and the spatial parameter *Sha* and *Spd*, respectively. The parameters with the three different changing trends are listed in Table 6. It can be seen that majority significant parameters exhibit a similar trend to Type 1 shown in Figure 3(a).

By observing Fig. 3, an obvious singular point can be found at 10,000 cycles corresponding to Joint 1, which is probably caused by the limited measurements. If the distortions caused by Joint 1 are ignored, corrected trends are proposed where the red dashed curves could be seen in Fig. 3. And the major nonlinear trends have become smoother after the correction. It can be noticed that most of the trends are non-monotonic and a transition point occurs at Joint 4, i.e., 26,000 cycles. Type 1 trend has an early descending until joint 4, and followed by a fast recovery, while Type 3 is a contrary version of Type 1. Type 2 is like a cubic form and the inflexions happen to be at Joints 2 and 4.

Table 6 Three typical trends of the significant surface topography parameters with the degeneration of osteoarthritis.

Type 1	*Sp*	*Spk*	*Smc*	*Vmp*	*S5p*	*Sv*	*Svk*	*Sxp*	*Vvv*	*S5v*	*Sk*	*Vmc*	*Vvc*	*Sz*	*S10z*	*Sq*	*Sa*	*Sdr*	*Sdv*	*Shv*
Type 2	*Sha*	*Sda*																		
Type 3	*Spd*																			

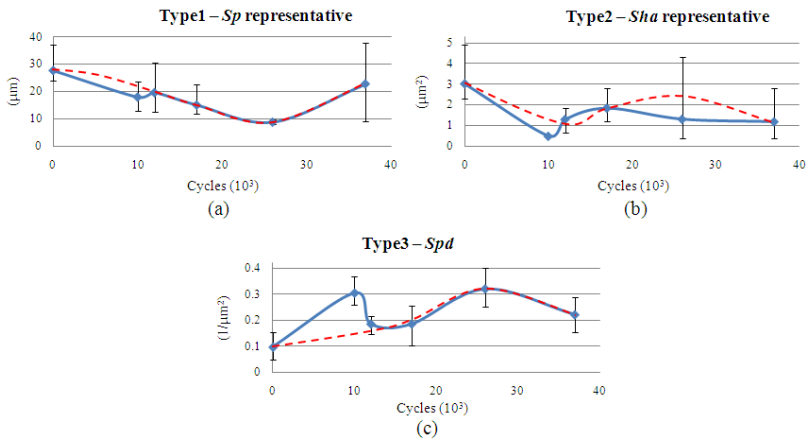

Fig. 3. The three typical trends (blue solid curves) of the wear particles surface topography parameters with degeneration of OA and their corrected trends (red dashed curves). The error bar is determined by the maximum and minimum parameter values within each group.

4.3 Correlation analysis

A correlation process was carried out to find out those parameters which are highly correlated with each other; thus they could be rationally pruned for selection of independent indicators. The correlation coefficients are listed in Table 7 in which the values between -0.7~0.7 are highlighted in yellow. It is known that a high correlation coefficient indicates that the two computed parameters are highly correlated and thus one of them should be selected. The following points have been made after performing the correlation analysis.

1. All the height related parameters and the hybrid parameter *Sdr* are highly correlated. *Sdr* has relatively low correlation with all the spatial and other hybrid parameters.
2. All the spatial parameters (*Sda*, *Sha*, *Spd*) and the two hybrid parameters (*Sdv*, *Shv*) are highly correlated. Among them,
    1) The spatial parameters *Sda* and *Sha* are particularly highly correlated; but both of them are less correlated with all the height related parameters and the hybrid parameter *Sdr*.
    2) Feature density *Spd* is less correlated with most height related parameters except *S5p*, *Svk*, *Sxp*, *Vvv*, *S5v*, *Sk*, *S10z* and the hybrid parameter *Sdr*, among which it can be noticed that most of them are valley height-related. This is understoodable because *Spd* describes the property related to the number of peaks on a defined surface.
    3) Hybrid parameters *Sdv* and *Shv* are particularly highly correlated. Unlike most spatial parameters, both of them are correlated with most height related parameters except *Svk*, *Sxp*, *Vvv*, *S5v* and the hybrid parameter *Sdr*.
3. The central regionalised high coefficients (grey-coloured) in Table 7 indicate that the classified parameters are self-correlated. It is correspondingly demonstrated that systematic parameter classification is rational.

Table 7 Correlation coefficients of the 23 significant parameters and the low-value coefficients which are between -0.7 and 0.7 are highlighted. For page size reason, all values are presented in one decimal precision.

	Height related																	***Hybrid***	***Spatial***			***Hybrid***	
	Sp	*Spk*	*Smc*	*Vmp*	*S5p*	*Sv*	*Svk*	*Sxp*	*Vvv*	*S5v*	*Sk*	*Vmc*	*Vvc*	*Sz*	*S10z*	*Sq*	*Sa*	*Sdr*	*Sda*	*Sha*	*Spd*	*Sdv*	*Shv*
Sp	1	1	0.9	1	1	0.9	0.7	0.8	0.8	0.7	0.8	0.9	0.9	1	0.9	0.9	0.9	0.7	0.4	0.5	-0.8	0.9	0.9
Spk	1	1	0.9	1	1	0.9	0.7	0.8	0.8	0.6	0.8	0.9	1	1	0.9	0.9	0.9	0.6	0.5	0.6	-0.9	0.9	0.9
Smc	0.9	0.9	1	0.9	1	1	0.8	0.9	0.9	0.8	1	1	1	1	0.9	1	1	0.8	0.5	0.5	-0.8	0.9	0.9
Vmp	1	1	0.9	1	1	0.9	0.7	0.8	0.8	0.7	0.8	0.9	1	1	0.9	0.9	0.9	0.7	0.5	0.6	-0.8	0.9	0.9
S5p	1	1	1	1	1	1	0.8	0.9	0.9	0.8	0.9	0.9	1	1	1	1	1	0.8	0.4	0.4	-0.7	0.8	0.9
Sv	0.9	0.9	1	0.9	1	1	0.9	1	1	0.9	1	1	1	1	1	1	1	0.9	0.3	0.3	-0.6	0.7	0.7
Svk	0.7	0.7	0.8	0.7	0.8	0.9	1	1	1	0.9	0.9	0.9	0.8	0.8	0.9	0.9	0.8	1	0	0.1	-0.4	0.6	0.5

Sxp	0.8	0.8	0.9	0.8	0.9	1	1	1	1	1	1	1	0.9	0.9	1	0.9	0.9	1	0.2	0.2	-0.5	0.7	0.6
Vvv	0.8	0.8	0.9	0.8	0.9	1	1	1	1	0.9	0.9	0.9	0.9	0.9	1	0.9	0.9	1	0.1	0.2	-0.5	0.6	0.6
S5v	0.7	0.6	0.8	0.7	0.8	0.9	0.9	1	0.9	1	0.9	0.9	0.8	0.8	0.9	0.8	0.8	1	0	0	-0.3	0.5	0.5
Sk	0.8	0.8	1	0.8	0.9	1	0.9	1	0.9	0.9	1	1	0.9	0.9	0.9	1	1	0.9	0.3	0.3	-0.6	0.8	0.7
Vmc	0.9	0.9	1	0.9	0.9	1	0.9	1	0.9		1	1	1	0.9	1	1	1	0.9	0.4	0.4	-0.7	0.8	0.8
Vvc	0.9	1	1	1	1	1	0.8	0.9	0.9	0.8	0.9	1	1	1	0.9	1	1	0.8	0.5	0.6	-0.8	0.9	0.9
Sz	1	1	1	1	1	1	0.8	0.9	0.9	0.8	0.9	0.9	1	1	1	1	1	0.8	0.4	0.4	-0.7	0.8	0.9
S10z	0.9	0.9	0.9	0.9	1	1	0.9	1	1	0.9	0.9	1	0.9	1	1	1	1	0.9	0.2	0.3	-0.6	0.8	0.8
Sq	0.9	0.9	1	0.9	1	1	0.9	0.9	0.9	0.8	1	1	1	1	1	1	1	0.8	0.5	0.5	-0.8	0.9	0.9
Sa	0.9	0.9	1	0.9	1	1	0.8	0.9	0.9	0.8	1	1	1	1	1	1	1	0.8	0.5	0.5	-0.8	0.9	0.8
Sdr	0.7	0.6	0.8	0.7	0.8	0.9	1	1	1	1	0.9	0.9	0.8	0.8	0.9	0.8	0.8	1	0	0	-0.3	0.5	0.5
Sda	0.4	0.5	0.5	0.5	0.4	0.3	0	0.2	0.1	0	0.3	0.4	0.5	0.4	0.2	0.5	0.5	0	1	1	-0.8	0.8	0.8
Sha	0.5	0.6	0.5	0.6	0.4	0.3	0.1	0.2	0.2	0	0.3	0.4	0.6	0.4	0.3	0.5	0.5	0	1	1	-0.8	0.8	0.8
Spd	-0.8	-0.9	-0.8	-0.8	-0.7	-0.6	-0.4	-0.5	-0.5	-0.3	-0.6	-0.7	-0.8	-0.7	-0.6	-0.8	-0.8	-0.3	-0.8	-0.8	1	-0.9	-0.9
Sdv	0.9	0.9	0.9	0.9	0.8	0.7	0.6	0.7	0.6	0.5	0.8	0.8	0.9	0.8	0.8	0.9	0.9	0.5	0.8	0.8	-0.9	1	1
Shv	0.9	0.9	0.9	0.9	0.9	0.7	0.5	0.6	0.6	0.5	0.7	0.8	0.9	0.9	0.8	0.9	0.8	0.5	0.8	0.8	-0.9	1	1

The correlation analysis results have assisted in selecting key parameters to be detailed in Section 4.4.

4.4 Relations to articular cartilage surfaces and key parameters

Since the wear particles were generated from the articular cartilage surfaces in knee joint wear processes, a correlation analysis was executed to investigate the correlation of the surface changes of the articular cartilages [52] and those of the wear particles characterised using the significant parameters. Only those significant parameters which could reveal the correlation have been selected as key parameters for wear particles analysis. It has been stated that selection of the significant parameters which have functional correlations is difficult [58, 59]. It is widely accepted that the selected key parameters should be stable and representative, i.e. capable of representing three typical trends. Therefore, one approach is to choose one key parameter from each type of trends in Table 6. Meanwhile, the p-values in the ANOVA analysis can also be an important indicator referring to significance level.

In the earlier articular cartilage surface characterisation, 24 significant parameters and 10 key parameters have been selected [52]. These 10 key parameters may only be limited in OA study through cartilage surfaces texture studies. Similarly, the described three typical trends and their representative wear debris key parameters above may only be useful as the references in particles analysis. A correlation between the 23 wear particles surfaces significant parameters and the 24 articular cartilage surfaces significant parameters was carried out in this session to determine key parameters for both cartilage and particles evaluations.

The correlation matrix is listed in Table 8 with the corresponding correlated parameters highlighted. It is noticeable that all the peak height related parameters of articular cartilage surfaces are normally highly correlated with the valley height related parameters of wear particle surfaces. And all the valley height related parameters of cartilage surfaces also have a strong reverse correlation with the particle surfaces. This evidence indicates wear particles and cartilage surfaces were ever directly contacted and had replicated surface textures. Using the following process methods, the key parameters are determined.

1. Divide all articular cartilage and wear particles significant parameters into three basic classes and subclasses as in Table 4 based on their definitions. The classification can assist to extract correct independent parameters.

2. The parameters which only exist in particles significant parameter list or in cartilage significant parameter list are neglected in the evaluation of both articular cartilage and wear particle surfaces. Remove them from the significant parameters list. As presented in Table 8, the shadowed parameters are removed.
3. Select one key parameter from each classified parameter group based on their corresponding correlation coefficients (grey coloured units) for the rest significant indicators. For example, *S5p* is selected as one key parameter because the correlation coefficient 0.4 is highest among all the coefficients in the peak height related parameters. Finally *S5p*, *Sv*, *Vvc*, *S10z*, *Sq*, *Sdr* and *Sda* are determined as the 7 key indicators. And 3 of them are feature parameters which are *S5p*, *S10z* and *Sda*.

Table 8 Correlation of the surface topography significant parameters between the wear particles and articular cartilage samples. For each parameter, the corresponding highest correlative parameters are highlighted; for the reason of page size, all the values are presented in one decimal precision.

WP(23) / AC(24)		***Height related***																	***Hybrid***	***Spatial***		***Hybrid***	
		Sp	*Spk*	*Smc*	*Vmp*	*S5p*	*Sv*	*Svk*	*Sxp*	*Vvv*	*S5v*	*Sk*	*Vmc*	*Vvc*	*Sz*	*S10z*	*Sq*	*Sa*	*Sdr*	*Sda*	*Sha*	*Spd*	*Sdv*	*Shv*
Height related	*Sp*	-0.3	-0.3	-0.4	-0.3	-0.4	-0.4	-0.5	-0.5	-0.5	-0.4	-0.4	-0.4	-0.4	-0.4	-0.4	-0.4	-0.4	-0.5	-0.4	-0.4	0.1	-0.5	-0.5
	Spk	-0.3	-0.2	-0.3	-0.2	-0.3	-0.3	-0.4	-0.4	-0.4	-0.3	-0.3	-0.3	-0.3	-0.3	-0.3	-0.3	-0.3	-0.4	-0.4	-0.3	0.0	-0.5	-0.4
	Smc	-0.3	-0.2	-0.2	-0.2	-0.3	-0.2	-0.3	-0.3	-0.3	-0.2	-0.2	-0.2	-0.2	-0.3	-0.3	-0.2	-0.2	-0.3	-0.3	-0.2	-0.1	-0.4	-0.4
	Vmp	-0.3	-0.2	-0.3	-0.2	-0.3	-0.3	-0.4	-0.4	-0.4	-0.3	-0.3	-0.3	-0.3	-0.3	-0.3	-0.3	-0.3	-0.4	-0.4	-0.3	0.1	-0.5	-0.4
	S5p	-0.3	-0.3	-0.4	-0.3	-0.4	-0.4	-0.6	-0.5	-0.5	-0.4	-0.4	-0.4	-0.4	-0.4	-0.4	-0.4	-0.4	-0.6	-0.4	-0.3	0.1	-0.5	-0.5
	Sv	-0.4	-0.4	-0.4	-0.4	-0.5	-0.4	-0.4	-0.4	-0.4	-0.3	-0.3	-0.4	-0.4	-0.4	-0.4	-0.4	-0.4	-0.4	-0.5	-0.5	0.2	-0.6	-0.6
	Svk	-0.3	-0.2	-0.2	-0.2	-0.3	-0.2	-0.2	-0.2	-0.2	-0.1	-0.1	-0.2	-0.2	-0.3	-0.2	-0.2	-0.2	-0.2	-0.5	-0.4	0.1	-0.5	-0.5
	Sxp	-0.2	-0.2	-0.1	-0.2	-0.2	-0.1	-0.2	-0.2	-0.2	-0.1	-0.1	-0.1	-0.2	-0.2	-0.2	-0.2	-0.2	-0.2	-0.4	-0.4	0.0	-0.4	-0.4
	Vvv	-0.3	-0.2	-0.2	-0.2	-0.3	-0.2	-0.2	-0.2	-0.2	-0.1	-0.1	-0.1	-0.2	-0.2	-0.2	-0.2	-0.2	-0.2	-0.4	-0.4	0.0	-0.5	-0.4
	S5v	-0.5	-0.4	-0.4	-0.4	-0.5	-0.4	-0.3	-0.4	-0.4	-0.3	-0.3	-0.4	-0.4	-0.4	-0.4	-0.4	-0.4	-0.3	-0.5	-0.5	0.2	-0.6	-0.6
	Sk	-0.2	-0.2	-0.2	-0.2	-0.3	-0.2	-0.3	-0.3	-0.3	-0.2	-0.2	-0.2	-0.2	-0.2	-0.3	-0.2	-0.2	-0.3	-0.3	-0.2	-0.1	-0.4	-0.4
	Vmc	-0.2	-0.2	-0.2	-0.2	-0.3	-0.2	-0.3	-0.2	-0.3	-0.2	-0.2	-0.2	-0.2	-0.2	-0.3	-0.2	-0.2	-0.3	-0.3	-0.2	-0.1	-0.4	-0.4
	Vvc	-0.2	-0.2	-0.2	-0.2	-0.3	-0.3	-0.4	-0.3	-0.3	-0.3	-0.2	-0.2	-0.2	-0.3	-0.3	-0.2	-0.2	-0.4	-0.3	-0.2	-0.1	-0.4	-0.4
	Sz	-0.4	-0.3	-0.4	-0.3	-0.4	-0.4	-0.4	-0.4	-0.5	-0.3	-0.4	-0.4	-0.4	-0.4	-0.4	-0.4	-0.4	-0.5	-0.5	-0.4	0.2	-0.6	-0.6
	S10z	-0.4	-0.4	-0.4	-0.4	-0.5	-0.4	-0.5	-0.4	-0.5	-0.4	-0.4	-0.4	-0.4	-0.4	-0.4	-0.4	-0.4	-0.5	-0.5	-0.4	0.2	-0.6	-0.6
	Sq	-0.3	-0.2	-0.2	-0.2	-0.3	-0.2	-0.3	-0.3	-0.3	-0.2	-0.2	-0.2	-0.2	-0.3	-0.3	-0.2	-0.2	-0.3	-0.4	-0.3	0.0	-0.4	-0.4
	Sa	-0.2	-0.2	-0.2	-0.2	-0.3	-0.2	-0.3	-0.3	-0.3	-0.2	-0.2	-0.2	-0.2	-0.2	-0.3	-0.2	-0.2	-0.3	-0.3	-0.3	0.0	-0.4	-0.4
	Ssk	0.1	0.0	-0.2	0.0	0.0	-0.3	-0.4	-0.4	-0.4	-0.4	-0.3	-0.2	-0.1	0.0	-0.2	-0.2	-0.2	-0.4	0.3	0.3	0.0	0.2	0.3
Hybrid	*Sdq*	-0.3	-0.2	-0.2	-0.2	-0.3	-0.3	-0.3	-0.3	-0.3	-0.3	-0.2	-0.3	-0.2	-0.3	-0.3	-0.3	-0.3	-0.4	-0.3	-0.3	0.0	-0.5	-0.4
	Sdr	-0.3	-0.2	-0.2	-0.2	-0.3	-0.2	-0.2	-0.2	-0.2	-0.2	-0.2	-0.2	-0.2	-0.2	-0.3	-0.2	-0.2	-0.3	-0.3	-0.3	0.0	-0.4	-0.4
	Spc	-0.5	-0.4	-0.4	-0.4	-0.5	-0.5	-0.5	-0.5	-0.5	-0.5	-0.4	-0.4	-0.4	-0.5	-0.5	-0.4	-0.4	-0.5	-0.3	-0.3	0.1	-0.6	-0.5
Spatial	*Str*	-0.2	-0.2	-0.5	-0.3	-0.3	-0.6	-0.7	-0.7	-0.7	-0.7	-0.6	-0.5	-0.4	-0.3	-0.5	-0.5	-0.5	-0.7	0.2	0.2	0.1	-0.1	0.0
	Sda	0.3	0.2	0.4	0.3	0.4	0.6	0.8	0.7	0.8	0.7	0.6	0.5	0.4	0.4	0.6	0.5	0.5	0.9	-0.2	-0.3	0.1	0.1	0.1
	Sha	0.3	0.2	0.4	0.3	0.4	0.6	0.8	0.7	0.8	0.7	0.6	0.5	0.4	0.4	0.5	0.4	0.4	0.8	-0.2	-0.2	0.1	0.1	0.1

Among the 7 selected key parameters, the former 6 have Type 1 trend and *Sda* has Type 2 trend. No representative is selected for Type 3 trend as *Spd* is insignificant in articular cartilage parameters group. The determined results are partially coincident with the parallel cartilage surface analysis results in which 10 key parameters, *S5p*, *Sv*, *Vvc*, *Sz*, *Sa*, *Ssk*, *Str*, *Sha*, *Sdq*, *Spc* have been selected. In addition, the 7 selected key parameters have also covered the three typical cartilage parameters changing trends in which four typical trends are summarised. Therefore, 7 key parameters are proposed to be potentially useful in future OA study which are shown in Table 9.

Table 9 Seven key field and feature parameters selected in this study.

	Control	**Joint 1**	**Joint 2**	**Joint 3**	**Joint 4**	**Joint 5**

	Mean	S. D.	Mean	S. D.	Mean	S. D.	Mean	S. D.	Mean	S. D.	Mean	S. D.
S5p (μm)	18.62	7.71	11.46	3.34	13.09	5.62	9.79	3.18	5.12	1.43	17.31	9.44
Sv (μm)	18.15	1.68	14.32	2.79	14.51	3.86	13.78	6.43	8.98	2.04	19.79	8.38
Vvc ($\mu m^3/mm^2$)	7.70E+6	2.24E+6	5.04E+6	5.53E+5	5.47E+6	1.69E+6	5.66E+6	2.07E+6	3.18E+6	5.32E+5	7.07E+6	3.19E+6
S10z (μm)	28.96	7.87	22.03	5.35	21.34	6.61	18.36	6.03	10.62	2.16	30.80	15.71
Sq (μm)	5.88	1.51	3.94	0.57	4.20	1.32	4.26	1.60	2.38	0.26	5.67	2.50
Sdr (%)	6.78E+3	5.19E+3	5.89E+3	1.01E+3	4.55E+3	1.89E+3	4.81E+3	3.31E+3	2.24E+3	7.44E+2	1.11E+4	7.37E+3
Sda (μm^2)	2.71	0.70	0.43	0.06	0.90	0.41	1.66	0.50	1.23	1.53	1.00	1.05

5. Discussion

In parallel to the articular cartilage surface study project [52], the field and feature parameter sets defined in ISO/FDIS 25178-2 have been applied to study the surface topography of wear particles samples generated in sheep knee joints under the different Osteoarthritis (OA) grades. Based on the significance and correlation analyses as well as the definitions of the numerical parameters, 7 key surface topography parameters have been finally determined for characterising the distinct wear features of the wear particles. The key parameters are *Sv*, *Vvc*, *Sq*, *Sdr*, *S5p*, *S10z* and *Sda*, of which the first four are field parameters and the remaining three are feature parameters from the height related and spatial groups as shown in Table 4.

Together with surface topography analysis, boundary morphology has also been studied to evaluate existing results. Compared with previous synovial joint particles boundary morphology studies, the average values of the parameters have a similar changing configuration at certain wear experiment phase [49]. For example, the area and length of the particles increase initially at the early stage of the wear test and then reduce at Joint 3 or 4, which complies with the whole wear process of former study. The reason s probably because the duration or intensity of wear test is longer or stronger than previous research. Meanwhile, the wear particles dimensions are apparently smaller than study of [49] but comparable with test of [30]. Therefore, more tests are needed to validate the synovial joint wear particle boundary morphology alteration for OA assessment in future research.

Unique to existing studies on wear particles using the conventional field parameters, this project has, for the first time, applied the feature parameters on the surface characterisations of synovial joint wear particles. This group of parameters uses novel pattern recognition techniques which ensure that targeted surface features could be examined verisimilarly [41-43]. In addition, from material and tribological aspects, the feature parameters are normally considered being highly functional relevance and stable to target surface [41, 55]. The above merits of the feature parameters have been confirmed in this study by the ANOVA results demonstrating that 8 of the total 9 feature parameters have significance with the wear debris surface modification under the wear progression. This positive outcome of the feature parameters has shown their significance in surface characterisation. Thus, it is believed that, based on the innovative pattern recognition techniques, the feature parameters implemented in this study have described functional properties of the wear particle surface topography.

Three basic changing trends of the significant parameters from Type 1 to Type 3 in OA degeneration are observed. They are respectively represented by *Sp*, *Sha* and *Spd* as shown in Fig 3. It worth to mention that majority of the confident parameters which are 20 of 23 have shown a Type 1 trend in Fig. 3(a). For example, the Type 1 trend representative parameter, *Sp* describing the largest height value within definition area, has shown a downward trend until Joint 4, and turned to a upward trend with Joint 5. Parameters having common Type 1 trend includes all height related parameters describing both peak and vale textures within defined surface area and hybrid parameters which also contain height relevant information. This Type 1 trend illustrates a smoothing wear history as wear test initiates and roughing transition at late OA stage. This observed trend is consistent with certain previous research findings of sheep joints wear debris characterised by the surface texture fractal dimension [34]. Work in [34] has reported that the fractal dimension of the particles surface texture reduces initially in the early stage of the wear test and then increases with the further extending of the testing duration.

The wear particle surface texture alteration trend found in this study is inconsistent with certain other former particle surfaces topography studies [30, 37]. In those previous researches, the morphologies of particle surfaces were observed to gradually become rougher from the Control joint to Joint 4, with a drop in the surface roughness at Joint 5. However, this research indicates that the wear debris surface roughness shown on Type 1 changing trend has a steady decrease until Joint 4 and then a reverse happens. Only the density of peak of *Spd* has an upward parabolic trend. The inconsistence may mainly be caused by the different numerical operations, such as the clipping process, levelling and filtration used in the data analyses. As Laser Scanning Confocal Microscopy (LSCM) images would capture target's entire surface information containing form, roughness, waviness, etc. Levelling and filtration would remove unnecessary dimension information such as unsteadily distributed large scale components [51, 53]. However, due to different images process technique, these steps were not carried out in the early researches.

The correlation of the changes in the wear particle surfaces topography and that of the articular cartilage samples has been conducted. The correlation matrix shown in Table 8 indicates the two surfaces have a tight inherent relationship, reflecting the origination and nature of the wear debris. According to the observed trends of both the samples, the particles and cartilage surface textures primarily evolve in a similar parabolic way, however, with entirely inverted directions. The study of the cartilage surfaces has revealed that the cartilage surface becomes rougher at the beginning of the wear process, and then is smoothened as the test cycle increases. For example, *S5p* of the cartilage surfaces, representing the average value of five peaks height information within a defined area, gains an increase until the worn joint 3. Synchronously, the wear debris surface texture undergoes a smoothening process at the early stage of the wear testing. And its surface asperity grows coarser and more irregular as the wear test moves to the late stage. This change is revealed by the trend of *Svk* of the wear particles, the most correlated parameter with *S5p* for the cartilage surfaces with a correlation coefficient of 0.6. The trend of *Svk* in Figure 3(a) shows that the average valley value in an equivalent area reduces from the particles generated from the control joint to the particles of Joint 4 subjected to the 26,000 testing cycles.

The above inverted relevance relationship may indicate that the wear particles are potentially replica products of the cartilage surfaces. To interpret and understand the trends, the structure of the articular cartilage has to be examined along with the wear process. The cartilage has the zoned structure mainly consisting of collagen and proteoglycan aggregates [8-10, 60]. In the superficial zone, collagen bundles dominantly align in the direction of the cartilage surface and interlace to form a very stable and elastic structure to support the surface while the downward zones are calcified and very stiff [31, 61]. At an early wear test stage, the crown part is torn away and lamellar like particles are released into the synovial fluid. This type of particles is not very rigid and may be subject to secondary wear in a three-bode wear mode. Their surface morphology thus may be modified, likely becoming smoother. As the wear test continuing, wear and tear progresses to a deep zone where calcified cellular materials or subchondral bone fragments are generated. For the above reason, at the heavily worn joints (corresponding to joints with OA grades 2 or 3), more prominent bony and chunky particles could be located [12-15, 34]. These particles generated at an advanced wear phase are rougher and also stiffer than those generated at the early stage. Since the cartilage wear process is very complicated and its wear mechanism is not fully understood at present, the results generated in this research may open a door for future research on a further understanding of wear processes and wear mechanism of synovial joints.

Although this project has demonstrated a new approach for the surface characterisation of wear particles in 3D, further work needs to be carried out to refine the techniques presented in this paper and to verify the trends. Firstly, the current clipping procedure cannot fully separate a wear particle from its background because of the irregularity of the wear particles boundary features. Some background noise usually remains and affects the surface characterisation as illustrated in Fig. 2(a). The negative factor cannot be solved at present and the induced error should be considered cautiously. To achieve an automated OA diagnostic, a stable recognition technique of wear debris regions is required. Topographic pattern recognition technique is thought to be a potential solution, however, the testing results have shown difficulties for this purpose [41, 62]. Therefore, a further development of

intelligent techniques is required. Secondly, considering the experimental data is limited, a robust validation with a large amount of experimental data needs to be carried out in the future.

6. Conclusion

In this research, the field and feature parameters defined in ISO/FDIS 25178-2, have been implemented to investigate the surface texture alteration of the synovial fluid wear particles under the three OA grades. 23 of the total 32 parameters, including the majority of the newly defined feature parameters have shown significance. Through a series of correlation analyses and selection process, 7 key parameters have been ultimately determined for characterising the distinct wear features of the particle surfaces. Compared with simultaneous articular cartilage studies, closed correlation and inverted trend coexist between the cartilage and particles surfaces textures changing under OA development. The complex, unexpected trends need to be further understood. These feature parameters are the first time to be used for evaluating the surface topography of the wear particles collected from sheep knee joints. The outcome has shown that the feature parameters have potential to be used for studying the functional properties of the particle surfaces for future OA assessment and diagnosis. To validate and understand the functional correlation of the surface topography indicators and OA conditions, further researches and experiments are needed in the future.

7. Acknowledgements

The authors would like to acknowledge Australian Research Council (ARC) research grant DP1093975, the University of Huddersfield under the excellent research programme and the European Research Council under its programme ERC-2008-AdG 228117-Surfund for their support to this project.

References

[1] T. Karachalios, A. Zibis, P. Papanagiotou, A.H. Karantanas, K.N. Malizos, N. Roidis, MR imaging findings in early osteoarthritis of the knee, European Journal of Radiology, 50 (2004) 225-230.
[2] T.E. McAlindon, C. Cooper, J.R. Kirwan, P.A. Dieppe, Knee pain and disability in the community, British Journal of Rheumatology, 31 (1992) 189-192.
[3] C. Cooper, S. Snow, T.E. McAlidon, S. Kellingray, B. Stuart, D. Coggon, P.A. Dieppe, Risk factors for the incidence and progression of radiographic knee osteoarthritis, Arthritis&Rheumatism, 43 (2000) 995-1000.
[4] C. Yuan, Z. Jin, J.L. Tipper, X. Yan, Numerical surface characterization of wear debris from artificial joints using atomic force microscopy, Chinese Science Bulletin, 54 (2009) 4583-4588.
[5] J.L. Tipper, P.J. Firkins, E. Ingham, J. Fisher, M.H. Stone, R. Farrar, Quantitative analysis of the wear and wear debris from low and high carbon content cobalt chrome alloys used in metal on metal total hip replacements, Journal of Material Science: Materials in Medicine, 10 (1999) 353-362.
[6] H. Kotlarz, C.L. Gunnarsson, H. Fang, J.A. Rizzo, Insurer and out-of-pocket costs of osteoarthritis in the US: Evidence from national survey data, Arthritis & Rheumatism, 60 (2009) 3546-3553.
[7] J.W. Ewing, Articular cartilage and knee joint function: Basic science and arthroscopy, Raven Press, New York, 1990.
[8] T.C.B. Pollard, S.E. Gwilym, A.J. Carr, The assessment of early osteoarthritis, Journal of Bone and Joint Surgery [Br], 90-B (2008) 411-421.
[9] A.K. Jeffery, G.W. Blunn, C.W. Archer, G. Bentley, Three-dimensional collagen architecture in bovine articular cartilage, Journal of Bone and Joint Surgery [Br], 73-B (1991) 795-801.
[10] P.K. Levangie, C.C. Norkin, Joint structure and function: A comprehensive analysis, 4th ed., F. A. Davis Company, Philadelphia, 2005.
[11] W.P. Chan, P. Lang, M.P. Stevens, K. Sack, S. Majumdar, D.W. Stoller, C. Basch, H.K. Genant, Osteoarthritis of the knee: Comparison of radiography, CT and MR imaging to assess extent and severity, American Journal of Roentgenology, 157 (1991) 799-806.

[12] P. Podsiadlo, M. Kuster, G.W. Stachowiak, Numerical analysis of wear particles from non-arthritic and osteoarthritic human knee joints, Wear, 210 (1997) 318-325.
[13] K. Mendel, N. Eliaz, I. Benhar, D. Hendel, N. Halperin, Magnetic isolation of particles suspended in synovial fluid for diagnostics of natural joint chondropathies, Acta Biomaterialia, 6 (2010) 4430-4438.
[14] M.S. Kuster, P. Podsiadlo, G.W. Stachowiak, Shape of wear particles found in human knee joints and their relationship to osteoarthritis, British Journal of Rheumatology, 37 (1998) 978-984.
[15] G.W. Stachowiak, P. Podsiadlo, Analysis of wear particle boundaries found in sheep knee joints during *in vitro* wear tests without muscle compensatoin, Journal of Biomechanics, 30 (1997) 415-419.
[16] H. Lipshitz, R. Etheredge, M.J. Glimcher, In vitro wear of articular cartilage, Journal of Bone and Joint Surgery, 57 (1975) 527-534.
[17] G.C. Ballantine, G.W. Stachowiak, The effects of lipid depletion on osteoarthritic wear, Wear, 253 (2002) 385-393.
[18] J.P. Pelletier, J. Martel-Pelletier, Therapeutic targets in osteoarthritis: from today to tomorrow with new imaging technology, Annals of the Rheumatic Diseases, 62 (2003) 79-82.
[19] J.C. Buckland-Wright, Quantitative radiography of osteoarthritis, Annals of the Rheumatic Diseases, 53 (1994) 268-275.
[20] C.P. Sabiston, M.E. Adams, D.K.B. Li, Magnetic resonance imaging of osteoarthritis: correlation with gross pathology using an experimental model, Journal of Orthopaedic Research, 5 (1987) 164-172.
[21] P. Ravaud, X. Ayral, M. Dougados, Radiologic progression of hip and knee osteoarthritis, Osteoarthritis and Cartilage, 7 (1999) 222-229.
[22] C.Y. Duan, A.A.E. Orás, S. Shott, H.S. An, G.B.J. Andersson, J.Z. Hu, H.B. Lu, N. Inoue, *In vivo* measurement of the subchondral bone thickness of lumbar facet joint using magnetic resonance imaging, Osteoarthritis and Cartilage, 19 (2011) 96-102.
[23] C.W. Jones, D. Smolinski, C. Willers, P.J. Yates, A. Keogh, D. Fick, T.B. Kirk, M.H. Zheng, Laser scanning confocal arthroscopy of a fresh cadaveric knee joint, Osteoarthritis and Cartilage, 15 (2007) 1388-1396.
[24] P. Podsiadlo, G.W. Stachowiak, 3-D imaging of surface topography of wear particles found in synovial joints, Wear, 230 (1999) 184-193.
[25] C.W. Jones, D. Smolinski, A. Keogh, T.B. Kirk, M.H. Zheng, Confocal laser scanning microscopy in orthopaedic research, Progress in Histochemistry and Cytochemistry, 40 (2005) 1-71.
[26] Z. Peng, T.B. Kirk, Z.L. Xu, The development of three-dimensional imaging techniques of wear particle analysis, Wear, 203-204 (1997) 418-424.
[27] R.V. Anamalay, T.B. Kirk, D. Panzera, Numerical descriptors for the analysis of wear surfaces using laser scanning confocal microscopy, Wear, 181-183 (1995) 771-776.
[28] D.N. Hanlon, I. Todd, E. Peekstok, W.M. Rainforth, S.v.d. Zwaag, The application of laser scanning confocal microscopy to tribological research, Wear, 251 (2001) 1159-1168.
[29] C.J.R. Sheppard, D.M. Shotton, Confocal Laser Scanning Microscopy, BIOS Scientific Publishers, Oxford, 1997.
[30] Z. Peng, Osteoarthritis diagnosis using wear particle analysis technique: Investigation of correlation between particle and cartilage surface in walking process, Wear, 262 (2007) 630-640.
[31] J.P. Wu, T.B. Kirk, Z. Peng, K. Miller, M.H. Zheng, Utilization of two-dimensional fast fourier transform and power spectral analysis for assessment of early degeneration of articular cartilage, Journal of Musculoskeletal Research, 9 (2005) 119-131.
[32] L. Lucas, N. Gilbert, D. Ploton, N. Bonnet, Visualization of volume data in confocal microscopy: comparison and improvements of volume rendering methods, Journal of Microscopy, 181 (1996) 238-252.
[33] T.V. Vorburger, J. Raja, Surface finish metrology tutorial, National Inst. of Standards and Technology, 1990.
[34] T.B. Kirk, Wear in synovial joints, in, University of Western Australia, Perth, 1992, pp. 211-212,226.
[35] P. Podsiadlo, G.W. Stachowiak, The development of the modified Hurst orientation transform for the characterization of surface topography of wear particles, Tribology Letters, 4 (1998) 215-229.
[36] G.W. Stachowiak, Numerical characterization of wear particles morphology and angularity of particles and surfaces, Tribology International, 31 (1998) 139-157.

[37] Z. Peng, M. Fasiolo, K. Hart, Investigation into changes in collagen structure of articular cartilage and wear particles of knee joints for osteoarthritic wear assessment, Journal of Musculoskeletal Research, 12 (2009) 143-152.
[38] X. Jiang, P.J. Scott, D.J. Whitehouse, L. Blunt, Paradigm shifts in surface metrology. Part II. The current shift, Proceedings of the Royal Society A 463 (2007) 2071-2099.
[39] P.J. Scott, Feature parameters, Wear, 266 (2009) 548-551.
[40] ISO, ISO/FDIS 25178-2, in: Geometrical product specification (GPS) - Surface texture: areal - part 2: terms, definitions and surface texture parameters, 2010.
[41] P.J. Scott, Pattern analysis and metrology: the extraction of stable features from observable measurements, Proceedings of the Royal Society A 460 (2004) 2845-2864.
[42] P.J. Scott, An algorithm to extract critical points from lattice height data, International Journal of Machine Tools and Manufacture, 41 (2001) 1889-1897.
[43] G.W. Wolf, A FORTRAN subroutine for cartographic generalization, Computers & Geosciences, 17 (1991) 1359-1381.
[44] L. Blunt, X. Jiang, Advanced techniques for assessment surface topography, Kogan Page Limited, 2003.
[45] J. Katta, Z. Jin, E. Ingham, J. Fisher, Biotribology of articular cartilage-A review of the recent advances Medical Engineering & Physics, 30 (2008) 1349-1363.
[46] G.W. Stachowiak, A.W. Batchelor, L.J. Griffiths, Friction and wear changes in synovial joints, Wear, 171 (1994) 135-142.
[47] G. Verberne, Y. Merkher, G. Halperin, A. Maroudas, I. Etsion, Techniques for assessment of wear between human cartilage surfaces, Wear, 266 (2009) 1216-1223.
[48] P. Podsiadlo, G.W. Stachowiak, Numerical analysis of shape of wear particles from arthritic and asymptomatic synovial joints, Journal of Orthopaedic Rheumatology, 8 (1995) 155-160.
[49] S.L. Graindorge, G.W. Stachowiak, Changes occurring in the surface morphology of articular cartilage during wear, Wear, 241 (2000) 143-150.
[50] G.S. Sodhi, J. Kaur, R.K. Garg, L. Kobilinsky, A fingerprint powder formulation based on rhodamine B dye, Journal of Forensic Identification, 53 (2003) 551-555.
[51] ISO, ISO/DIS 25178-3, in: Geometrical product specification (GPS) - Surface texture: areal - part 3: Specification operators, 2008.
[52] Y. Tian, J. Wang, Z. Peng, X. Jiang, Numerical analysis of cartilage surfaces for osteoarthritis diagnosis using field and feature parameters, in: The 18th International Conference on Wear of Material, Elsevier, Philadelphia US, 2011.
[53] ISO, ISO 11562, in: Geometrical Product Specifications (GPS) -- Surface texture: Profile method -- Metrological characteristics of phase correct filters, 1996.
[54] S. Xiao, F. Xie, L. Blunt, P. Scott, X. Jiang, Feature extraction for structured surface based on surface networks and edge detection, Materials Science in Semiconductor Processing, 9 (2006) 210-214.
[55] J. Wang, X. Jiang, E. Gurdak, P. Scott, R. Leach, P. Tomlins, L. Blunt, Numerical characterisation of biomedical titanium surface texture using novel feature parameters, Wear, 271 (2011) 1059-1065.
[56] B.G. Tabachnick, L.S. Fidell, Using Multivariate Statistics, 4th ed., Allyn and Bacon, 2000.
[57] K.J. Stout, L. Blunt, W.P. Dong, E. Mainsah, N. Luo, T. Mathia, P.J. Sullivan, H. Zahouani, Development of Methods for the Characterisation of Roughness in Three Dimensions, Office for official publications of the European Communities, Luxembourg, 1993.
[58] P.M. Lonardo, H. Trumpold, L.D. Chiffre, Progress in 3D Surface Microtopography Characterization, CIRP Annals - Manufacturing Technology, 45 (1996) 589-598.
[59] L.D. Chiffre, P. Lonardo, H. Trumpold, D.A. Lucca, G. Goch, C.A. Brown, J. Raja, H.N. Hansen, Quantitative characterisation of surface texture, CIRP Annals - Manufacturing Technology, 49 (2000) 635-642, 644-652.
[60] T. Aigner, J. Stöve, Collagens-major component of the physiological cartilage matrix, major target of cartilage degeneration, major tool in cartilage repair, Advanced Drug Delivery Reviews, 55 (2003) 1569-1593.

[61] J.P. Wu, Development of Microscopic Technique for Study of the 3D Collagen Structure in the Superficial Zone and It's relationship to the Degeneration of Articular Cartilage, in, University of Western Australia, Perth, 2006.
[62] S. Takahashi, T. Ikeda, Y. Shinagawa, T.L. Kunii, M. Ueda, Algorithms for Extracting Correct Critical Points and Constructing Topological Graphs from Discrete Geographical Elevation Data, Computer Graphics Forum, 14 (1995) 181-192.